Characterization of a type-2 diacylglycerol acyltransferase from *Haematococcus pluvialis* reveals possible allostery of the recombinant enzyme

Trinh Nguyen [a,b], Yang Xu [a], Mona Abdel-Hameed [c], John L. Sorensen [c], Stacy D. Singer [d], Guanqun Chen [a,b,*]

[a] Department of Agricultural, Food and Nutritional Science, University of Alberta, Edmonton, Alberta, Canada, T6G 2P5

[b] Department of Biological Sciences, University of Manitoba, Winnipeg, Manitoba, Canada, R3T 2N2

[c] Department of Chemistry, University of Manitoba, Winnipeg, Winnipeg, Manitoba, Canada, R3T 2N2

[d] Agriculture and Agri-Food Canada, Lethbridge Research and Development Centre, Lethbridge, Alberta, Canada, T1J 4B1

*To whom correspondence should be addressed. Phone: (+1) 780-492-4265, gc24@ualberta.ca (G. Chen)

Keywords: DGAT; Algae; *Haematococcus pluvialis*; Triacylglycerol biosynthesis; Sigmoidal kinetics; *Saccharomyces cerevisiae*

Abbreviations

DAG, Diacylglycerol; DGAT, Diacylglycerol acyltransferase; ER, Endoplasmic reticulum; GC, Gas chromatography; TAG, Triacylglycerol; TLC, Thin layer chromatography

Abstract:

Haematococcus pluvialis is a green microalga used in the algal biotechnology industry that can accumulate considerable amounts of storage triacylglycerol (TAG) and astaxanthin, which is a high-value carotenoid with strong antioxidant activity, under stress conditions. Diacylglycerol acyltransferase (DGAT) catalyzes the last step of the acyl-CoA-dependent TAG biosynthesis and appears to represent a bottleneck in algal TAG formation. In this study, putative *H. pluvialis DGAT2* cDNAs (*HpDGAT2A*, *B*, *D* and *E*) were identified from a transcriptome database and were subjected to sequence-based *in silico* analyses. The coding sequences of *HpDGAT2B*, *D* and *E* were then isolated and characterized through heterologous expression in a TAG-deficient *Saccharomyces cerevisiae* strain H1246. The expression of *HpDGAT2D* allowed the recovery of TAG biosynthesis in this yeast mutant, and further *in vitro* enzymatic assays confirmed that the recombinant HpDGAT2D possessed strong DGAT activity. Interestingly, the recombinant HpDGAT2D displayed sigmoidal kinetics in response to increasing acyl-CoA concentrations, which has not been reported in plant or algal DGAT2 in previous studies.

Introduction

Plant oil is the major energy storage compound in oilseeds, and has been widely used as a source of food, feed, and renewable material for diverse industrial applications (Xu et al., 2018a). The global demand for plant oils has been consistently increasing over the past five decades and is expected to continue rising due to our increasing population and reliance on plant oil-derived compounds (Chen et al., 2015b). As such, there is currently intense interest in improving oil production in well-established oil crops, as well as exploring novel sources of oil production, such as oleaginous microalgae. Indeed, microalgae provide an important alternative source for industrial oil production due to their rapid growth, simple cultivation conditions, high oil content and value-added secondary metabolites.

Haematococcus pluvialis is a green microalga widely known for its ability to synthesize the highest amount of astaxanthin, which is a red-colored carotenoid with strong antioxidant ability and important commercial value, in nature. Under stress conditions, this compound can constitute up to 4% of its cell weight (Lorenz and Cysewski, 2000; Chekanov et al., 2014). This microalga also represents a potential source of oil, since a considerable increase in oil content accompanies the accumulation of astaxanthin (Zhekisheva et al., 2002b; Ambati et al., 2014). Although the exact mechanisms behind stress-induced oil and astaxanthin accumulation in *H. pluvialis* are not well-understood, several lines of evidence have suggested that the biosynthesis pathways of both compounds appears to be linked through the regulation of oil biosynthetic enzymes (Gwak et al., 2014; Chen et al., 2015a; Zhekisheva et al., 2002a). Indeed, the accumulation of astaxanthin appears to be dependent on the accumulation of oil since the introduction of specific inhibitors of oil biosynthetic enzymes to algal cultures leads to substantial decreases in both compounds (Chen et al., 2015a).

Triacylglycerol (TAG) is the major constituent of plant and microalgal oils, and is composed of three fatty acids esterified to a glycerol backbone. TAG is synthesized in the endoplasmic reticulum

(ER) through the acyl-CoA-dependent or independent pathways (Chen et al., 2015b; Bates et al., 2013; Bates, 2016). Diacylglycerol acyltransferase (DGAT; EC 2.3.1.20) catalyzes the final acylation of *sn*-1,2-diacylglycerol (DAG) to form TAG, which is the last and only committed step in the acyl-CoA-dependent TAG formation (Chapman and Ohlrogge, 2012; Xu et al., 2018a). This enzyme appears to represent a bottleneck in TAG biosynthesis in some oilseed crops and algal species and thus has been regarded as a key target in manipulating oil production (Liu et al., 2012; Xu et al., 2018a). In plants and algae, there are two major membrane-bound forms of DGAT, designated DGAT1 and DGAT2, which share no sequence similarity (Xu et al., 2018a). DGAT1 appears to be the dominant player in TAG accumulation in many plants, whereas DGAT2 may have an important role in the formation of TAG containing unusual fatty acids (Li et al., 2010; Xu et al., 2018a, 2018b). In microalgae, only one copy of *DGAT1* has been identified in a number of microalgal species, whereas multiple copies of *DGAT2* genes are typically present (Chen and Smith, 2012), suggesting that *DGAT2* may play an important function in TAG biosynthesis and algal growth.

In this study, the possible functions of DGAT2 from *H. pluvialis* (HpDGAT2) was explored via *in silico* analysis and *in vitro* and *in vivo* characterization. The coding regions encoding three putative DGAT2 enzymes (HpDGAT2B, D and E) were isolated from *H. pluvialis* and expressed in *Saccharomyces cerevisiae* H1246, which is a quadruple mutant devoid of TAG biosynthetic ability, in order to assess their capacities to recover TAG biosynthesis. The activities and kinetics of HpDGAT2D was then further characterized using an *in vitro* system.

Materials and methods

Sequence analysis

Putative *HpDGAT2* sequences were identified by conducting a Blast search against the *H. pluvialis* Transcriptome Shotgun Assembly Sequence Database (GenBank accession number

SRR1040551) (Gwak et al., 2014) using *Arabidopsis thaliana DGAT2* (*AtDGAT2*) and *Chlamydomonas reinhardtii* DGAT2 genes (*CreDGAT2A*, *B*, *D*, and *E*) as queries. The partial sequences identified were used to design primers for the isolation of the full-length cDNA of each candidate *HpDGAT2* (described below), which were used in the following analyses. The theoretical molecular weight and isoelectric point values of the deduced HpDGAT2 were calculated using the Compute pI/Mw server (http://web.expasy.org/compute_pi/, accessed on March 7, 2019). The identity and similarity of amino acid sequences were determined using MatGAT (version 2.01) (Campanella et al., 2003). Multiple candidate sequence alignments of DGAT2 from different species were performed using ClustalW with the default settings in MEGA7 software (Kumar et al., 2016). The alignment was then used to construct a neighbour-joining tree using the same software with the *Poisson* model and pairwise deletion with 1000 bootstrap repetitions. Transmembrane domains and sequence logos on signature motifs of HpDGAT2 proteins were predicted using TMHMM (Krogh et al., 2001) and WebLogo (http://weblogo.berkeley.edu/logo.cgi, accessed on March 7, 2019), respectively.

Haematococcus pluvialis growth and HpDGAT2 cDNAs isolation

The green alga *H. pluvialis* (UTEX 2505) was obtained from the culture collection of algae at the University of Texas at Austin. The alga was grown in 250 mL Erlenmeyer flasks containing 50 mL bold basal medium at 22°C and 50 µmol photons/m^2/s (low light) with a 12:12h photoperiod. Exponentially growing cells with a cell density of approximately 1.5×10^5 cells/mL were subjected to high-light stress conditions where the light intensity was raised to 150 µmol photons/m^2/s continuously. For the isolation of candidate *HpDGAT2* coding regions, algal cells were collected after 24 h of high-light stress, and used for total RNA extraction using the Spectrum™ Plant Total RNA Kit (Sigma-Aldrich, Oakville, Canada). Total RNA was converted to cDNA using the Maxima First-Strand cDNA

Synthesis Kit (Thermo Fisher, Waltham, MA), and the resulting cDNA was then used as template for the isolation of the candidate *HpDGAT2* coding regions using the primers listed in Table 1.

Heterologous expression of cDNAs encoding HpDGAT2 in yeast mutant H1246

The isolated coding regions of the putative *HpDGAT2* genes were subcloned into the pYES2.1/V5-His-TOPO vector (Invitrogen). After the identity of each sequence was confirmed *via* sequencing, individual constructs were transformed into the *S. cerevisiae* mutant H1246 using the S.C EasyComp^{TM} Transformation Kit (Invitrogen). Yeast transformants were first grown in liquid minimal medium [0.67% (w/v) yeast nitrogen base, 0.2% (w/v) SC-Ura] containing 2% (w/v) raffinose], which was then used as a seed culture to inoculate liquid minimal medium containing 2% (w/v) galactose and 1% (w/ v) raffinose at an initial OD600 value of 0.4.

Analyses of yeast lipids

Yeast lipids were analyzed using gas chromatography (GC) as previously described (Xu et al., 2019). Briefly, yeast total lipids were extracted from 20 mg of lyophilized yeast cells with 100 μg of triheptadecanoin (17:0 TAG) added as an internal standard. Yeast cells were homogenized with 1 mL of chloroform:methanol:0.9% NaCl (2:1:0.9; v/v/v) mixture in the presence of 0.5 mm glass beads by a bead beater (Biospec, Bartlesville, OK, USA). The chloroform phase was collected and concentrated under nitrogen. The extracted total lipids were isolated on thin layer chromatography (TLC) plates (SIL G25, 0.25mm, Macherey-Nagel, Germany) using the mobile phase of hexane/diethyl ether/acetic acid (80:20:1, v/v/v). The TAG bands were visualized using primulin stain, scraped into tubes, and trans-methylated using 1 mL of 3 N methanolic HCl at 80ºC for 1 h. The resulting fatty acid methyl esters were extracted twice with hexane, dried under nitrogen gas and resuspended in 1 mL of hexane before

being subjected to GC analysis. GC analysis was performed with an Agilent GC 6890N (Agilent Technologies, Wilmington, DE, USA) as described previously (Xu et al., 2019).

Preparation of yeast microsomal fractions

Microsomal fractions were isolated from recombinant yeast cells as described previously (Xu et al., 2017). Yeast cells were collected after 12 h induction by centrifugation at 3000 g for 5 min at 4 °C and were resuspended in 1 mL of lysis buffer containing 20 mM Tris-HCl pH 7.9, 10 mM $MgCl_2$, 1 mM EDTA, 5% v/v glycerol, 300 mM ammonium sulfate and 2 mM DTT, followed by lysis with bead beating (Biospec, Bartlesville, OK). The cell lysate was first centrifuged at 10,000 g at 4 °C for 20 min to remove cell debris and then the supernatant was further centrifuged at 100,000 g for 70 min to pellet the microsomal fractions. The microsomal fractions were recovered and resuspended in suspension buffer containing 3 mM imidazole pH 7.4 with 125 mM sucrose and stored at -80 ºC. The protein concentration in the microsomal fraction was determined using the Bradford assay (Bradford, 1976).

In vitro DGAT activity assay

DGAT assays were performed as previously described (Xu et al., 2017). In brief, the 60-µL reaction mixture contained 200 mM HEPES-NaOH (pH 7.4), 3.2 mM $MgCl_2$, 333 µM *sn*-1,2- diolein dispersed in 0.2% (v/v) Tween 20, 15 µM [1-^{14}C] oleoyl- CoA (55 µCi/µmol) (PerkinElmer, Waltham, MA) and 10 µg of microsomal proteins. The reaction was initiated by adding the microsomal proteins containing recombinant HpDGAT2, incubated at 30 °C with shaking for 1 h, and was then stopped with 10 µL of 10% (w/v) SDS. Fifty microliters of the reaction mixture were spotted on TLC plates and developed in hexane/diethyl ether/ acetic acid (80:20:1, v/v). The TAG bands were visualized using a Typhoon Trio Variable Mode Imager (GE Healthcare, Chicago, IL) and radioactive activity was quantified using an LS 6500 multi-purpose scintillation counter (Beckman-Coulter, Brea, CA).

For enzyme kinetic studies, DGAT activity was examined with oleoyl-CoA concentrations varying from 0.1 to 15 μM and *sn*-1,2-diolein concentration held constant at 333 μM. Kinetic parameters were calculated by fitting the enzyme activity data to the Michaelis-Menten or allosteric sigmoidal equation using GraphPad (Prism version 6.0; GraphPad Software, La Jolla, CA).

Results

Haematococcus pluvialis has four putative HpDGAT2 isoforms with divergent phylogenetic relationships

To identify the putative sequences encoding DGAT2 enzymes from *H. pluvialis*, the sequences of *DGAT2* homologs from model plant and algal species including *A. thaliana* (*AtDGAT2*) and *C. reinhardtii* (*CrDGAT2A*, *B*, *D*, and *E*) were used to query the Transcriptome Shotgun Assembly Sequence Database of *H. pluvialis* (SRR1040551) (Gwak et al., 2014). Four putative *DGAT2* cDNAs were identified from *H. pluvialis* (Table 2) and were designated *HpDGAT2A, B, D* and *E* based on homology to *CrDGAT2.* HpDGAT2A, B, D, and E share 52.3%, 51.6%, 72.8% and 64.2% amino acid similarity with CrDGAT2A, B, D and E, respectively (Table 3). Consistent with previous reports, the putative HpDGAT2 have basic isoelectric points (9.54-9.86), and up to 2 predicted transmembrane domains each (Table 2) (Cao, 2011; Xu et al., 2019).

To explore the evolutionary distribution of *H. pluvialis* DGAT2 isoforms, phylogenetic analysis was performed using the protein sequences of HpDGAT2 and DGAT2 from *A. thaliana* (AtDGAT2), *Homo sapiens* (HsDGAT2), *Mus musculus* (MmDGAT2), *S. cerevisiae* (ScDGAT2), *C. reinhardtii* (CreDGAT2) and *Chromochloris zofingiensis* (CzDGAT2) (Fig. 1). As expected, DGAT2 from terrestrial plants and animals are separated into different clades, with yeast DGAT2 grouping with animal DGAT2 (Fig. 1). *H. pluvialis* has one plant-like DGAT2 (HpDGAT2A), one animal-like

DGAT2 (HpDGAT2B), and two other DGAT2 (HpDGAT2D and E) belonging to a separate clade, which is unique to microalgae (algal clade).

The conserved functional motifs of different HpDGAT2 isoforms were further analyzed (Fig. 2). The YFP motif, which is highly conserved among animal and plant DGAT2 enzymes, is well-conserved among algal DGAT2 enzymes that fall within the plant-like and animal-like clades, but is less conserved in those isoforms falling within the algal DGAT2 clade, where it instead comprises YFR/H/K (Fig. 2). Similarly, the HPHG motif found in animal DGAT2 proteins and the corresponding EPHS motif found in plant DGAT2 proteins are also highly conserved among algal DGAT2 that fall within the animal-like and plant-like clades, respectively. However, a motif closer in sequence to the animal-like HPHG motif (A/FPHG) is present in algal DGAT2 that fall within the algal clade. Finally, the RXGFX(K/ R)XAXXXGXX(L/V)VPXXXFG(E/Q) motif, which makes up the longest conserved sequence in plant and animal DGAT2, is also conserved among DGAT2 isoforms from green algae.

HpDGAT2D is able to recover TAG biosynthesis in yeast strain H1246

To verify the function of the putative HpDGAT2 enzymes, coding regions encoding HpDGAT2B, D, and E were isolated and expressed in the *S. cerevisiae* H1246 mutant (*MATα are1*-Δ::HIS3, *are2*-Δ::*LEU2, dga1*-Δ::*KanMX4, Iro1*-Δ::*TRP1*). This yeast mutant strain contains knockout mutations in four TAG biosynthesis-related genes (*dga1, lro1, are1,* and *are2*) and is unable to synthesize TAG (Sandager et al., 2002). The ability of this mutant to synthesize TAG can be recovered through the introduction of an active DGAT. As shown in Fig. 3A, HpDGAT2D was able to restore yeast TAG biosynthesis, where the transformed yeast generated large amounts of TAG, comprising 1.5% and 2.6% of the dry weight after 24 and 72 h induction, respectively. In contrast, no TAG was detected in *HpDGAT2B*, *HpDGAT2E*, and *LacZ* transformed yeast. Further fatty acid composition analysis suggests that the TAG isolated from yeast producing HpDGAT2D comprised

large amounts of unsaturated fatty acids (~80%, 18:1 and 16:1) and only small amounts of saturated fatty acids (~20%, 18:0 and 16:0) (Fig. 3B).

HpDGAT2D encodes an active DGAT and displays sigmoidal kinetics in response to increasing acyl-CoA concentration

Since HpDGAT2D was able to restore TAG accumulation in the yeast mutant H1246, the *in vitro* DGAT activity of HpDGAT2D was further analyzed using yeast microsomal fractions. As shown in Fig. 4A, HpDGAT2D was found to possess strong DGAT activity, whereas no detectable DGAT activity was observed in yeast microsomal fractions containing LacZ. To kinetically characterize HpDGAT2D, the microsomal enzyme activity of recombinant HpDGAT2D was assessed over a range of oleoyl-CoA concentrations. DGAT activity was augmented dramatically with increased oleoyl-CoA concentration (between 0.1 and 7.5 μM), and then remained stable with further increases in oleoyl-CoA concentration (Fig. 4B). The initial reaction velocity data from HpDGAT2D were fit to the Michaelis-Menten or allosteric sigmoidal equation, and the sigmoidal kinetics with a Hill coefficient value of 1.7 was found to be the preferred model for this enzyme (Fig. 4B). The apparent kinetic parameters were calculated using the allosteric sigmoidal equation, and the apparent V_{max} and $S_{0.5}$ values were found to be 133.0 ± 4.6 pmol TAG/min/mg protein and 1.33 ± 0.09 μM, respectively.

Discussion

H. pluvialis is able to produce a substantial amount of oil along with astaxanthin under stress conditions and has great potential as an alternative source for industrial oil production (Spolaore et al., 2006). Although the exact mechanisms of stress-induced oil and astaxanthin accumulation in *H. pluvialis* are largely unknown, their accumulation were found to be co-regulated by oil biosynthetic enzymes (Chen et al., 2015a). Therefore, understanding the stress-induced lipid biosynthetic pathways

is pivotal for the improvement in the production of both oil and astaxanthin in *H. pluvialis*. DGAT catalyzes the terminal step in acyl-CoA-dependent TAG production, and the expression of four *DGAT2* isoforms was found to be up-regulated in *H. pluvialis* under stress conditions (Ma et al., 2018a, 2018b), which suggests their possible involvement in stress-induced TAG accumulation. In the current study, we aim to identify the *DGAT2* cDNAs from the green algae *H. pluvialis* and functionally characterize the encoded enzymes using a yeast system.

Four HpDGAT2 isoforms (HpDGAT2A, B, D, and E) were identified from *H. pluvialis* (Table 2) and were found to separated into different clades, with HpDGAT2A grouping with plant DGAT2, HpDGAT2B grouping with animal DGAT2, and HpDGAT2D and E forming a unique clade (Fig. 1). Similarly, in the green algae *C. reinhardtii* and *C. zofingiensis*, at least one DGAT2 is clustered with plant DGAT2 (plant-like clade) and animal DGAT2 (animal-like clade), respectively, and more than two others fall into the algal clade (Fig. 1). Functional motif analysis suggests that the conserved motifs with potentially important functions, which have been previously identified in DGAT2 enzymes from plants, animals, fungi and microalgae (Liu et al., 2011; Chen and Smith, 2012), were also present in HpDGAT2 isoforms but with varying degrees of conservation (Fig. 2). Together, these results indicate the divergent distribution pattern of DGAT2 may broadly exist and have important physiological functions in green microalgae (Chen and Smith, 2012; Xu et al., 2019).

The cDNAs encoding HpDGAT2B, D and E were further isolated from *H. pluvialis* and transformed into yeast mutant H1246 for functional characterization. Only HpDGAT2D rather than HpDGAT2B and E were able to restore the TAG biosynthesis ability of yeast mutant H1246 (Fig. 3A). HpDGAT2D shares 57.2% pairwise identity at the amino acid level with CreDGAT2D (Table 3), and they both belong to the algal DGAT2 clade (Fig. 1). Within this clade, several members (including CreDGAT2D) have been reported previously to be capable of complementing oil biosynthesis in TAG-deficient yeast mutants (Hung et al., 2013; Xin et al., 2017; Sanjaya et al., 2013). The failure to restore

252 yeast TAG biosynthesis by expressing an algal or plant *DGAT2* has previously been reported (Wagner
253 et at., 2010), which may be caused by the differences in codon usage between yeast and algae/plants.
254 Indeed, Aymé et al. (2014) observed a strong codon bias affecting the expression of Arabidopsis
255 *DGAT2* in yeast. In addition, it is also possible that the functionality of heterologously expressed
256 *DGAT2* may be hindered by the limited fatty acid composition of yeast, which does not contain the
257 diverse species of fatty acids as algae and thus cannot provide appropriate substrates for DGAT.
258 Therefore, it will be interesting to further test the function of HpDGAT2B and E in yeast using codon-
259 optimized sequences or by providing appropriate exogenous fatty acids to the yeast culture.

260 The fatty acid composition of the resulting yeast TAG appears to be related to the substrate
261 specificity of the introduced DGAT2 towards the four dominant fatty acids in yeast. For instance, yeast
262 cells producing CreDGAT2D and DGAT2A from *Nannochloropsis oceanica* led to the accumulation
263 of about 20% and 40% of 16:0 in TAG, respectively, which may derive from their preference for 16:0-
264 CoA (Hung et al., 2013; Xin et al., 2017; Sanjaya et al., 2013). In the present study, the TAG isolated
265 from yeast producing HpDGAT2D contained ~80% of 18:1 and 16:1 and ~20% of 18:0 and 16:0 (Fig.
266 3B), suggesting that HpDGAT2D may have a lower preference for 16:0-containing substrate than the
267 two DGAT2 from *N. oceanica*, and a higher preference for monounsaturated fatty acids. In *H.*
268 *pluvialis*, the fatty acid composition of total lipids and TAG was changed when the algae cells were
269 subjected to light stress, in which 16:0, 18:1 and 18:2 increased with the concomitant decreases in 18:3
270 (Chen et al., 2016; Bilbao et al., 2016). Considering the up-regulation of all four *HpDGAT2* transcripts
271 under light stress (Ma et al., 2018a, 2018b), it is possible that different HpDGAT2 isoforms may
272 display different substrate preferences and thus contribute to altered algal fatty acid composition.
273 Indeed, *C. reinhardtii* DGAT2 have been demonstrated to contribute to the synthesis of diverse TAG
274 species in algal cells by displaying distinct specificities towards acyl-CoA and DAG (Liu et al., 2016).
275 Therefore, it is interesting to conduct a comprehensive *in vitro* characterization of HpDGAT2 with

different substrates including both acyl-CoA and DAG. The results would not only identify and compare the substrate specificity and selectivity of the DGAT2 isoforms, but also help to explain the physiological role of HpDGAT2 in affecting TAG fatty acid profiles of algal cells.

Further *in vitro* DGAT assay using yeast microsomal fractions containing HpDGAT2D confirmed that HpDGAT2D indeed encoded an active enzyme (Fig. 4A). Interestingly, HpDGAT2D was found to display sigmoidal kinetics in response to acyl-CoA (Fig. 4B), suggesting the enzyme was allosterically regulated by acyl-CoA (Caldo et al., 2017). Sigmoidal kinetics towards increasing acyl-CoA concentration have been identified in DGAT1 enzymes from different species (Xu et al., 2017; Roesler et al., 2016; Caldo et al., 2017) but not in DGAT2 enzymes prior to this study. The sigmoidal response of algal DGAT2 to acyl-CoA may be metabolically meaningful. Since DGAT2 is less active in the presence of low acyl-CoA levels, more acyl-CoA would be directed to membrane lipid biosynthesis for algal cell growth and division. Conversely, when the levels of acyl-CoA are high, DGAT2 activity would increase and algal cells would use more acyl-CoA for storage TAG assembly. Such positive cooperativity in HpDGAT2D could feasibly be caused by the presence of multiple substrate binding sites, where the binding of substrate at one site may enhance the binding affinity of substrate at another site (Caldo et al., 2017). However, limited information is currently available on the substrate binding features of DGAT2. One motif FLXLXXXn (n = nonpolar amino acid) was proposed for neutral lipid binding in mouse DGAT2 (Xu et al., 2018a), but it is not well-conserved in DGAT2 enzymes from plants and algae. In *Brassica napus* DGAT1, this type of positive cooperativity is likely mediated by the allosteric site in the hydrophilic N-terminal domain (Caldo et al., 2017). The N-terminal region in DGAT2, however, is short in length and has less conservation than that of DGAT1, which suggests that a different mechanism may be behind this phenomenon in DGAT2.

In summary, putative *HpDGAT2* isoforms with divergent phylogenetic distributions were identified from *H. pluvialis*, and coding regions of three of these isoforms (*HpDGAT2B*, *D* and *E*) were isolated and characterized in the yeast mutant H1246. HpDGAT2D was found to be capable of recovering TAG accumulation in H1246 mutant yeast, and *in vitro* enzyme characterization showed that this enzyme possesses strong DGAT activity. Further analysis indicated that HpDGAT2D was allosterically modulated by its substrate acyl-CoA. Intriguingly, our study reports the first observation of the positive cooperativity of DGAT2 with its substrate, which may help shed light on the biochemical characterization of other DGAT2 enzymes in both microalgae and higher plants, and also provides valuable information for engineering TAG biosynthesis in *H. pluvialis* and other oleaginous organisms in the future.

FUNDING SOURCES

The authors are grateful for the support provided by the University of Alberta Start-up Research Grant, Natural Sciences and Engineering Research Council of Canada Discovery Grants (RGPIN-2016-05926 to G.C.) and (RGPIN-2017-04958 to J.L.S.) and the Canada Research Chairs Program (G.C.).

CONFLICT OF INTEREST

The authors declare no conflict of interest.

AUTHOR CONTRIBUTIONS

G.C. conceived and supervised the research; G.C., Y.X., and T.N. designed the experiments; T.N. and Y.X. performed the experiments; all authors contributed to data analysis; Y.X., T.N., S.D.S. and G.C. wrote the article with contributions of all other authors.

References

Ambati, R., Phang, S.M., Ravi, S., and Aswathanarayana, R. (2014). Astaxanthin: Sources, extraction, stability, biological activities and its commercial applications—A review. Mar. Drugs 12: 128.

Aymé, L., Baud, S., Dubreucq, B., Joffre, F., and Chardot, T. (2014). Function and localization of the *Arabidopsis thaliana* diacylglycerol acyltransferase DGAT2 expressed in yeast. PLoS one 9: e92237.

Bates, P.D., Stymne, S., and Ohlrogge, J. (2013). Biochemical pathways in seed oil synthesis. Curr. Opin. Plant Biol. 16: 358-364.

Bates, P. D. (2016). Understanding the control of acyl flux through the lipid metabolic network of plant oil biosynthesis. BBA Mol. Cell Biol. L. 1861: 1214-1225.

Bilbao, P. G. S., Damiani, C., Salvador, G. A., and Leonardi, P. (2016). *Haematococcus pluvialis* as a source of fatty acids and phytosterols: Potential nutritional and biological implications. J. Appl. Phycol. 28: 3283-3294.

Bradford, M.M. (1976). A rapid and sensitive method for the quantitation of microgram quantities of protein utilizing the principle of protein-dye binding. Anal. Biochem. 72: 248–254.

Caldo, K.M.P., Acedo, J.Z., Panigrahi, R., Vederas, J.C., Weselake, R.J., Lemieux, M.J. (2017). Diacylglycerol acyltransferase 1 is regulated by its N-terminal domain in response to allosteric effectors. Plant Physiol. 175: 667–680.

Campanella, J.J., Bitincka, L., and Smalley, J. (2003). MatGAT : An application that generates similarity/identity matrices using protein or DNA sequences. BMC Bioinformatics 4: 29.

Cao, H. (2011). Structure-function analysis of diacylglycerol acyltransferase sequences from 70 organisms. BMC Res. Notes 4: 249.

Chapman, K.D. and Ohlrogge, J.B. (2012). Compartmentation of triacylglycerol accumulation in plants. J. Biol. Chem. 287: 2288–2294.

Chekanov, K., Lobakova, E., Selyakh, I., Semenova, L., Sidorov, R., and Solovchenko, A. (2014). Accumulation of astaxanthin by a new *Haematococcus pluvialis* strain BM1 from the white sea coastal rocks (Russia). Mar. Drugs 12: 4504–4520.

Chen, G., Wang, B., Han, D., Sommerfeld, M., Lu, Y., Chen, F., and Hu, Q. (2015a). Molecular mechanisms of the coordination between astaxanthin and fatty acid biosynthesis in *Haematococcus pluvialis* (*Chlorophyceae*). Plant J. 81: 95–107.

Chen, G., Woodfield, H.K., Pan, X., Harwood, J.L., and Weselake, R.J. (2015b). Acyl-trafficking during plant oil accumulation. Lipids 50: 1057–1068.

Chen, J.E. and Smith, A.G. (2012). A look at diacylglycerol acyltransferases (DGATs) in algae. J. Biotechnol. 162: 28–39.

Gwak, Y., Hwang, Y.S., Wang, B., Kim, M., Jeong, J., Lee, C.G., Hu, Q., Han, D., and Jin, E. (2014). Comparative analyses of lipidomes and transcriptomes reveal a concerted action of multiple defensive systems against photooxidative stress in *Haematococcus pluvialis*. J. Exp. Bot. 65: 4317–4334.

Hung, C.H., Ho, M.Y., Kanehara, K., and Nakamura, Y. (2013). Functional study of diacylglycerol acyltransferase type 2 family in *Chlamydomonas reinhardtii*. FEBS Lett. 587: 2364–2370.

Krogh, A., Larsson, B., von Heijne, G., and Sonnhammer, E. (2001). Predicting transmembrane protein topology with a hidden Markov model: Application to complete genomes. J. Mol. Biol. 305: 567–580.

Kumar, S., Stecher, G., and Tamura, K. (2016). MEGA7: Molecular Evolutionary Genetics Analysis version 7.0 for bigger datasets. Mol. Biol. Evol. 33: msw054.

Li, R., Yu, K., Hatanaka, T., and Hildebrand, D.F. (2010). *Vernonia* DGATs increase accumulation of epoxy fatty acids in oil. Plant Biotechnol. J. 8: 184–195.

Liu, J., Han, D., Yoon, K., Hu, Q., and Li, Y. (2016). Characterization of type 2 diacylglycerol

acyltransferases in *Chlamydomonas reinhardtii* reveals their distinct substrate specificities and functions in triacylglycerol biosynthesis. Plant J. 86: 3-19.

Liu, Q., Siloto, R.M.P., Lehner, R., Stone, S.J., and Weselake, R.J. (2012). Acyl-CoA:diacylglycerol acyltransferase: molecular biology, biochemistry and biotechnology. Prog. Lipid Res. 51: 350–377.

Liu, Q., Siloto, R.M.P., Snyder, C.L., and Weselake, R.J. (2011). Functional and topological analysis of yeast acyl-CoA:diacylglycerol acyltransferase 2, an endoplasmic reticulum enzyme essential for triacylglycerol biosynthesis. J. Biol. Chem. 286: 13115–13126.

Lorenz, R.T. and Cysewski, G.R. (2000). Commercial potential for *Haematococcus microalgae* as a natural source of astaxanthin. Trends Biotechnol. 18: 160–167.

Ma, R., Thomas-Hall, S.R., Chua, E.T., Alsenani, F., Eltanahy, E., Netzel, M.E., Netzel, G., Lu, Y., and Schenk, P.M. (2018a). Gene expression profiling of astaxanthin and fatty acid pathways in *Haematococcus pluvialis* in response to different LED lighting conditions. Bioresour. Technol. 250: 591–602.

Ma, R., Thomas-Hall, S.R., Chua, E.T., Eltanahy, E., Netzel, M.E., Netzel, G., Lu, Y., and Schenk, P.M. (2018b). Blue light enhances astaxanthin biosynthesis metabolism and extraction efficiency in *Haematococcus pluvialis* by inducing haematocyst germination. Algal Res. 35: 215–222.

Roesler, K., Shen, B., Bermudez, E., Li, C., Hunt, J., Damude, H.G., Ripp, K.G., Everard, J.D., Booth, J.R., Castaneda, L., Feng, L., and Meyer, K. (2016). An improved variant of soybean type 1 diacylglycerol acyltransferase increases the oil content and decreases the soluble carbohydrate content of soybeans. Plant Physiol. 171: 878–893.

Sandager, L., Gustavsson, M.H., Stahl, U., Dahlqvist, A., Wiberg, E., Banas, A., Lenman, M., Ronne, H., and Stymne, S. (2002). Storage lipid synthesis is non-essential in yeast. J Biol Chem 277: 6478–6482.

399 Sanjaya, Miller, R., Durrett, T.P., Kosma, D.K., Lydic, T.A., Muthan, B., Koo, A.J., Bukhman, Y. V,
400 Reid, G.E., Howe, G.A., Ohlrogge, J., and Benning, C. (2013). Altered lipid composition and
401 enhanced nutritional value of Arabidopsis leaves following introduction of an algal diacylglycerol
402 acyltransferase 2. Plant Cell 25: 677–693.
403 Spolaore, P., Joannis-Cassan, C., Duran, E., and Isambert, A. (2006). Commercial applications of
404 microalgae. J. Biosci. Bioeng. 101: 87–96.
405 Wagner, M., Hoppe, K., Czabany, T., Heilmann, M., Daum, G., Feussner, I., and Fulda, M. (2010).
406 Identification and characterization of an acyl-CoA: diacylglycerol acyltransferase 2 (DGAT2)
407 gene from the microalga *O. tauri*. Plant Physiol. Biochem. 48: 407-416.
408 Xin, Y., Lu, Y., Lee, Y.-Y.Y., Wei, L., Jia, J., Wang, Q., Wang, D., Bai, F., Hu, H., Hu, Q., Liu, J., Li,
409 Y., and Xu, J. (2017). Producing designer oils in industrial microalgae by rational modulation of
410 co-evolving type-2 diacylglycerol acyltransferases. Mol. Plant 10: 1523–1539.
411 Xu, Y., Caldo, K.M.P., Pal-Nath, D., Ozga, J., Lemieux, M.J., Weselake, R.J., and Chen, G. (2018a).
412 Properties and biotechnological applications of acyl-CoA:diacylglycerol acyltransferase and
413 phospholipid:diacylglycerol acyltransferase from terrestrial plants and microalgae. Lipids 53:
414 663–688.
415 Xu, Y., Chen, G., Greer, M.S., Caldo, K.M.P., Ramakrishnan, G., Shah, S., Wu, L., Lemieux, M.J.,
416 Ozga, J., and Weselake, R.J. (2017). Multiple mechanisms contribute to increased neutral lipid
417 accumulation in yeast producing recombinant variants of plant diacylglycerol acyltransferase 1. J.
418 Biol. Chem. 292: 17819–17831.
419 Xu, Y., Falarz, L., and Chen, G. (2019). Characterization of type-2 diacylglycerol acyltransferases in
420 the green microalga *Chromochloris zofingiensis*. J. Agric. Food Chem. 67: 291–298.
421 Xu, Y., Holic, R., Li, D., Pan, X., Mietkiewska, E., Chen, G., Ozga, J., Weselake, R.J., and Holic, R.
422 (2018b). Substrate preferences of long-chain acyl-CoA synthetase and diacylglycerol

acyltransferase contribute to enrichment of flax seed oil with α-linolenic acid. Biochem. J. 475: 1473–1489.

Zhekisheva, M., Boussiba, S., Khozin-Goldberg, I., Zarka, A., and Cohen, Z. (2002a). Accumulation of oleic acid in *Haematococcus pluvialis* (Chlorophyceae) under nitrogen starvation or high light is correlated with that of astaxanthin esters. J. Phycol. 38: 325–331.

Zhekisheva, M., Boussiba, S., Khozin-Goldberg, I., Zarka, A., and Cohen, Z. (2002b). Accumulation of triacylglycerols in *Haematococcus pluvialis* is correlated with that of astaxanthin esters. J. Phycol. 38: 40–41.

Figure legends

Fig. 1. Sequence analysis of putative DGAT2 enzymes from *H. pluvialis*. Phylogenetic relationship among putative DGAT2 enzymes from *H. pluvialis.* The neighbour-joining tree was constructed with the *Poisson* model and pairwise deletion with 1000 bootstrap repetitions. Bootstrap values are shown at the tree nodes. *Arabidopsis thaliana*, *At*; *Chlamydomonas reinhardtii*, *Cre*; *Chromochloris zofingiensis*, *Cz*; *Homo sapiens*, *Hs*; *Mus musculus*, *Mm*; *Saccharomyces cerevisiae*, *Sc*. The Phytozome/Genbank accession numbers for each protein sequence are as follows: AtDGAT2 (**NP_566952**), CreDGAT2A (**Cre03.g205050**), CreDGAT2B (**Cre12.g557750**), CreDGAT2C (**Cre02.g079050**), CreDGAT2D (**Cre06.g299050**), CreDGAT2E (**Cre09.g386912**), CzDGAT2A (**Cz08g14220**), CzDGAT2B (**Cz11g21100**), CzDGAT2C (**Cz11g24150**), CzDGAT2D (**Cz09g27290**), CzDGAT2E (**Cz15g22140**), CzDGAT2F (**Cz06g35060**), CzDGAT2G (**Cz06g22030**), HsDGAT2 (**AAK84176**), MmDGAT2 (**AAK84175**), and ScDGAT2 (**NP_014888**).

Fig. 2. Alignment of functional motifs within DGAT2 proteins. The partial protein sequence regarding HpDGAT2A is based on the partial coding sequence obtained from the Transcriptome Shotgun Assembly Sequence Database of *H. pluvialis*.

Fig. 3. Effect of heterologous *HpDGAT2* expression on the lipid contents of yeast strain H1246. A. Triacylglycerol (TAG) content of yeast producing HpDGAT2 after 24 and 72 h induction. B. Fatty acid composition of TAG isolated from yeast producing HpDGAT2D after 72 h induction. Data represent means ± SD, n=3. Asterisk indicates TAG content that significantly differs from the control ($P<0.05$). Statistical analysis was performed using the Student's t-test.

Fig. 4. *In vitro* microsomal DGAT activity of HpDGAT2D. A. Microsomal DGAT activity of HpDGAT2D. B. Sigmoidal kinetics of HpDGAT2D in response to increasing oleoyl-CoA concentration. The data were fit to a nonlinear regression using the allosteric sigmoidal equation (R^2 = 0.95). Plots were generated using GraphPad Prism. Data represent means ± S.D, n = 3. Asterisk indicates DGAT activity that significantly differs from the control ($P<0.05$). Statistical analysis was performed using the Student's t-test.

TABLE

Table 1. Primers used in the current study.

Names	Primer sequence (5' – 3')
HpDGAT2B – F	ATGGCTGGTGATACTGCGTCA
HpDGAT2B – R	TCACTGTACAAACTCCAGGCTCT
HpDGAT2D – F	AAGATGGGCGTTAAAAAGCCAG
HpDGAT2D – R	TCACTCGATGCTCAGCGG
HpDGAT2E – F	GAAATGGGTGTCGCAACGAAT
HpDGAT2E – R	TCACTGGATCTCCAGGGGCTT

Table 2. Overview of putative *DGAT2* sequences from *H. pluvialis*

Genes	ID	Coding sequence length (bp)	Protein length	Molecular mass (KDa)	Isoelectric point	Number of predicted transmembrane domain using TMHMM
*HpDGAT2A**	SRR1040551.29510	687	229	25.275	9.86	0
HpDGAT2B	SRR1040551.15574	1107	369	39.912	9.6	2
HpDGAT2D	SRR1040551.19876	990	330	37.606	9.54	2
HpDGAT2E	SRR1040551.6808	954	318	34.864	9.72	0

* Information regarding HpDGAT2A is predicted based on the partial coding sequence obtained from the Transcriptome Shotgun Assembly Sequence Database of *H. pluvialis* (SRR1040551).

Table 3. Amino acid sequence identity (%; italics) and similarity (%; bold) between DGAT2 from *H. pluvialis* and *C. reinhardtii* using MatGAT (Campanella et al., 2003).

	CreDGAT 2A	CreDGAT 2B	CreDGAT 2D	CreDGAT 2E	HpDGAT 2A	HpDGAT 2B	HpDGAT 2D	HpDGAT 2E
CreDGAT 2A		*29.5*	*27.6*	*29.4*	*39*	*26.1*	*27.1*	*30.4*
CreDGAT 2B	**50.2**		*26.1*	*27*	*22.5*	*35.9*	*25.8*	*26.3*
CreDGAT 2D	**46**	**44.5**		*50.1*	*21.7*	*23.6*	*57.2*	*40.6*
CreDGAT 2E	**48.6**	**46.8**	**67.1**		*23.4*	*27.2*	*48.6*	*47.7*
HpDGAT 2A	**52.3**	**35.3**	**33.5**	**38.6**		*21.5*	*21.6*	*25*
HpDGAT 2B	**40.5**	**51.6**	**42.7**	**45.4**	**32.1**		*22.6*	*25.3*
HpDGAT 2D	**49.5**	**45**	**72.8**	**70.5**	**34.3**	**41.3**		*39.8*
HpDGAT 2E	**47.1**	**44.7**	**56.6**	**64.2**	**40.4**	**40.2**	**63.5**	

Amino acid sequence identity

Amino acid sequence similarity

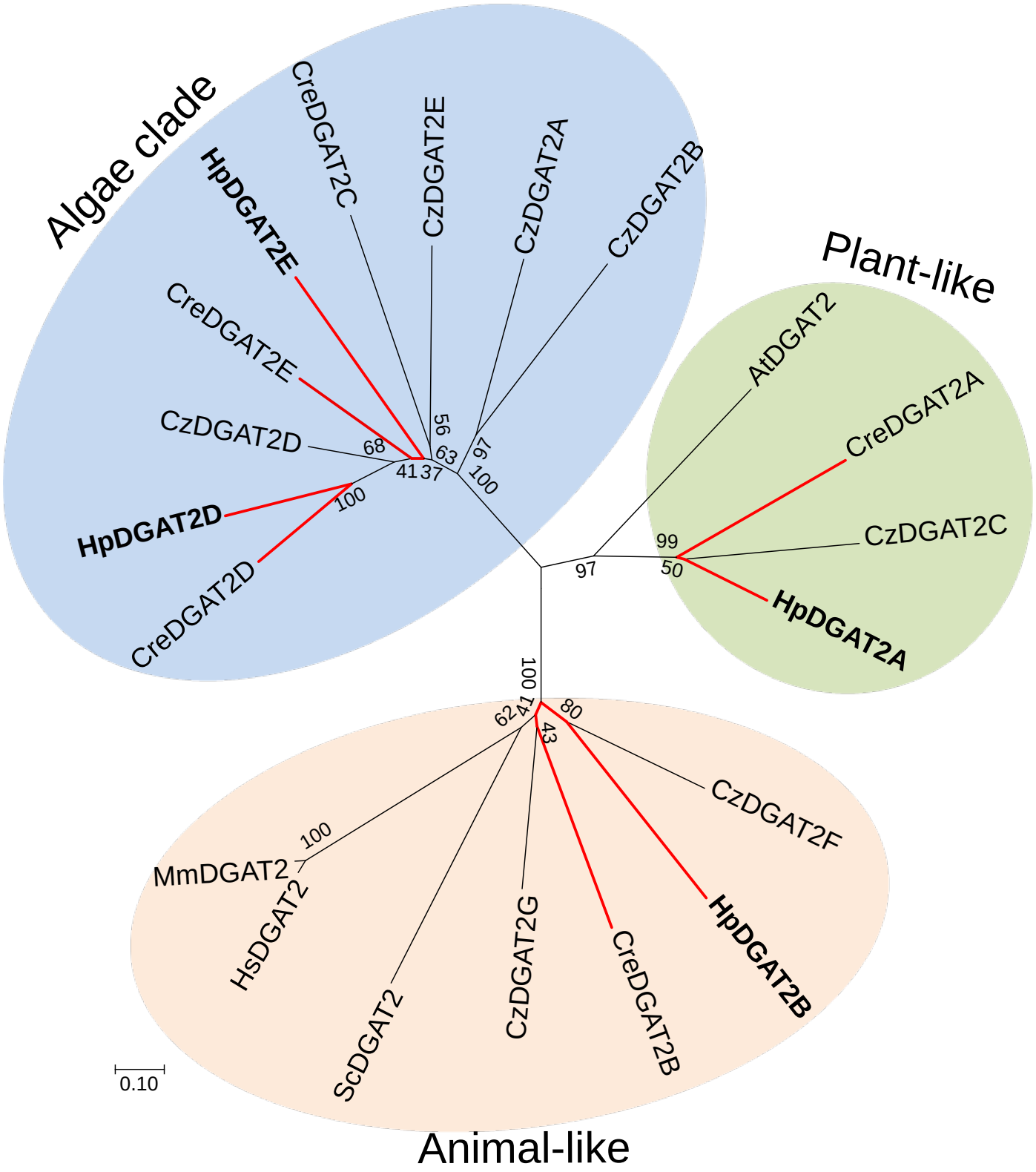
Algae clade
Plant-like
Animal-like
CreDGAT2C
CzDGAT2E
CzDGAT2A
CzDGAT2B
HpDGAT2E
CreDGAT2E
CzDGAT2D
HpDGAT2D
CreDGAT2D
AtDGAT2
CreDGAT2A
CzDGAT2C
HpDGAT2A
CzDGAT2F
MmDGAT2
HsDGAT2
ScDGAT2
CzDGAT2G
CreDGAT2B
HpDGAT2B
0.10

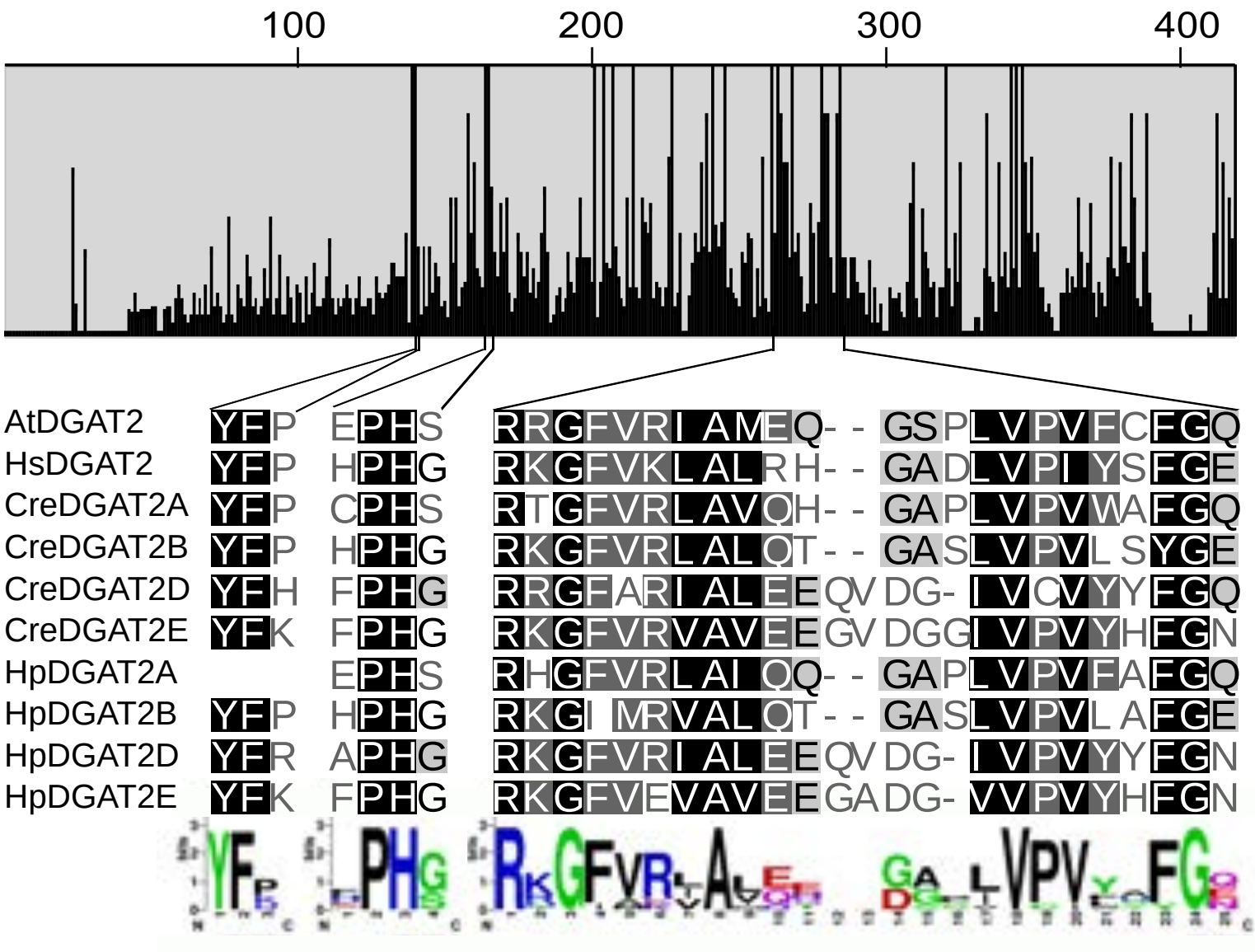
100
200
300
400
AtDGAT2 YFP EPHS RRGFVRIAMEQ- - GSPLVPVFCFGQ
HsDGAT2 YFP HPHG RKGFVKLALRH- - GADLVPIYSFGE
CreDGAT2A YFP CPHS RTGFVRLAVQH- - GAPLVPVWAFGQ
CreDGAT2B YFP HPHG RKGFVRLALQT- - GASLVPVLSYGE
CreDGAT2D YFH FPHG RRGFARIALEEQV DG- IVCVYYFGQ
CreDGAT2E YFK FPHG RKGFVRVAVEEGV DGGIVPVYHFGN
HpDGAT2A EPHS RHGFVRLAIQQ- - GAPLVPVFAFGQ
HpDGAT2B YFP HPHG RKGIMRVALQT- - GASLVPVLAFGE
HpDGAT2D YFR APHG RKGFVRIALEEQV DG- IVPVYYFGN
HpDGAT2E YFK FPHG RKGFVEVAVEEGA DG- VVPVYHFGN

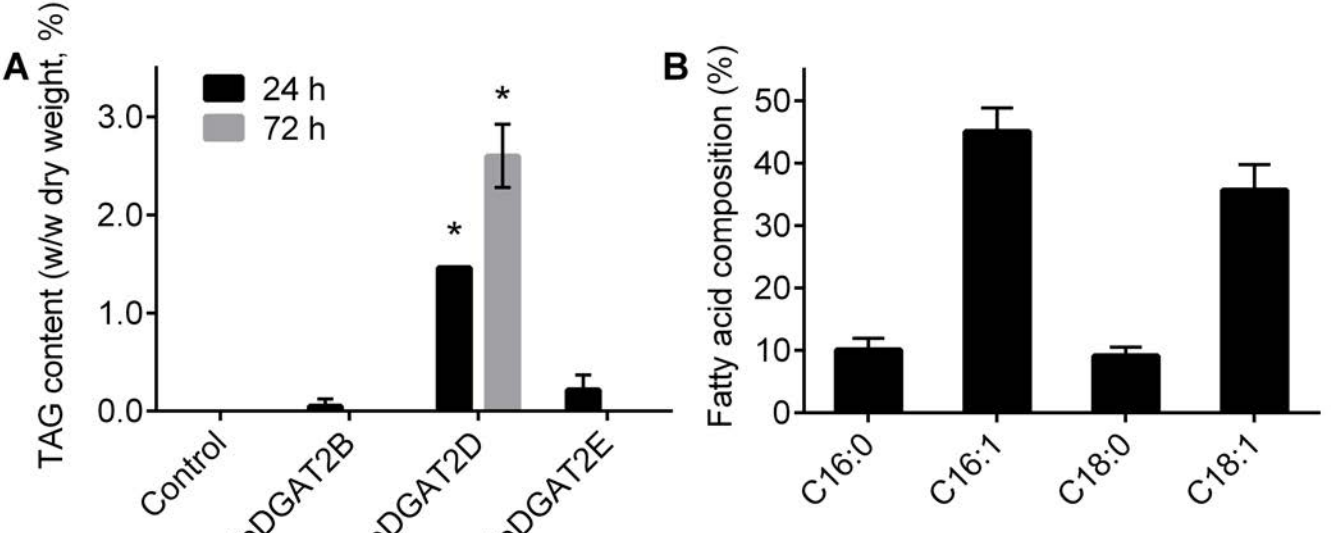
A
TAG content (w/w dry weight, %)
24 h
72 h
3.0
2.0
1.0
0.0
*
*
Control
HpDGAT2B
HpDGAT2D
HpDGAT2E
B
Fatty acid composition (%)
50
40
30
20
10
0
C16:0
C16:1
C18:0
C18:1

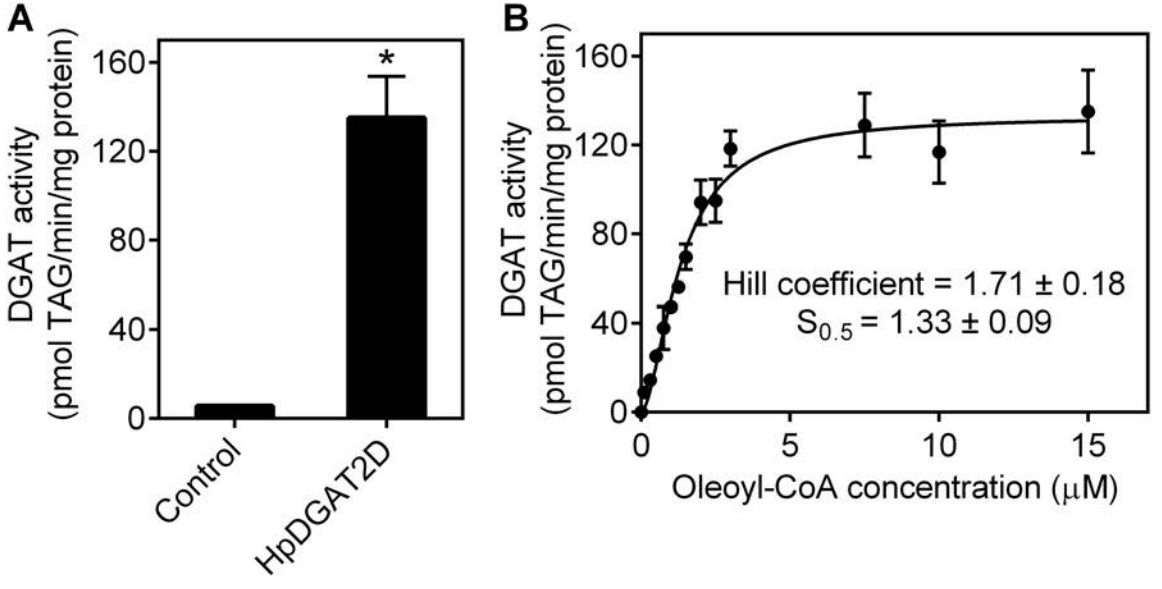
A
DGAT activity
(pmol TAG/min/mg protein)
160
120
80
40
0
*
Control
HpDGAT2D
B
DGAT activity
(pmol TAG/min/mg protein)
160
120
80
40
0
Hill coefficient = 1.71 ± 0.18
S0.5 = 1.33 ± 0.09
0
5
10
15
Oleoyl-CoA concentration (μM)